Journal of Economic Entomology, 112(3), 2019, 1274–1284
doi: 10.1093/jee/toz026
Research

Forest Entomology

Genetic Variability Among *Xyleborus glabratus* Populations Native to Southeast Asia (Coleoptera: Curculionidae: Scolytinae: Xyleborini) and the Description of Two Related Species

Anthony I. Cognato,[1,4] Sarah M. Smith,[1] You Li,[2] Thai Hong Pham,[3] and Jiri Hulcr[2]

[1]Department of Entomology, Michigan State University, 288 Farm Lane, Room 243, East Lansing, MI 48824, [2]School of Forest Resources and Conservation, University of Florida, 1745 McCarty Drive, Gainesville, FL 32611, [3]Vietnam National Museum of Nature, Vietnam Academy of Science and Technology, 18 Hoang Quoc Viet Street, Cau Giay, Hanoi, Vietnam, and [4]Corresponding author, e-mail: cognato@msu.edu

Subject Editor: Brian Sullivan

Received 28 September 2018; Editorial decision 25 January 2019

Abstract

The redbay ambrosia beetle, *Xyleborus glabratus* Eichhoff, is native to Southeast Asia, where it specializes on Lauraceae trees. It forms a symbiosis with the ambrosia fungus *Raffaelea lauricola* T.C. Harr., Fraedrich & Aghayeva, which can act as a pathogen in living host trees. The beetle and fungus were recently introduced into the United States, where they have killed millions of native Lauraceae trees and threaten the avocado industry. These introduced populations have limited genetic variation. In the native range, the fungi are genetically variable, but the native genetic variability of the beetles is unknown. It is important to assess the beetle's native genetic variation because different lineages may vary in the capacity to vector this fungus, which may affect disease etiology. Here, we analyzed genetic variation in several Chinese, Taiwanese, and Vietnamese populations of *X. glabratus* using mitochondrial (COI) and nuclear DNA (CAD) markers. Phylogenetic analysis revealed nine COI haplotypes and four CAD genotypes. Uncorrected 'p' distance for intrapopulation comparisons ranged from 0 to 0.1 and 0 to 0.013 and interpopulation comparisons ranged from 0.137 to 0.168 and 0.015 to 0.032 for COI and CAD, respectively. Two populations exceeded the range of intraspecific nucleotide differences for both genes. Given that individuals from these populations also exhibited consistent morphological differences, they are described as two new species: *Xyleborus insidiosus* Cognato & Smith, n. sp. and *Xyleborus mysticulus* Cognato & Smith, n. sp. *Xyleborus glabratus* was redescribed and a lectotype was designated to facilitate its recognition in light of these new species. These results indicate that *X. glabratus* is genetically variable and is related to two morphologically similar species. Whether these new species and *X. glabratus* lineages associate with different fungal strains is unknown. Given that the biology and host colonization of these new species are unknown, preventing their introduction to other regions is prudent.

Key words: Laurel wilt, invasive pest, ambrosia beetle

The redbay ambrosia beetle, *Xyleborus glabratus* Eichhoff, is an Asian endemic ambrosia beetle that was first detected in the Southeastern United States in 2002 (Rabaglia et al. 2006). *Xyleborus glabratus* vectors a symbiotic fungus, *Raffaelea lauricola* T.C. Harr., Fraedrich & Aghayeva, which is pathogenic to many species of Lauraceae trees and causes the systemic vascular disease laurel wilt. Within 16 yr of its discovery, the beetle and the fungus have colonized forests across nine Southeastern states and have killed over 300 million redbay, swampbay, and avocado trees (*Persea* Mill. spp.; Hughes et al. 2017, Formby et al. 2018). Although the beetle and fungus prefer *Persea* spp. as hosts, they have the potential to decimate sassafras trees [*Sassafras albidum* (Nutt.) Nees (Lauraceae)], which would increase their range into more northern latitudes (Hulcr and Lou 2013, Kendra et al. 2013, Formby et al. 2018). Based on the limited genetic variation found in the adventive populations of both the beetle and the fungus, it is likely that only a few individuals, perhaps a single one, founded the U.S. population (Hughes et al. 2017, Wuest et al. 2017). In contrast, the native populations of the fungus in Asia are genetically variable lending evidence for a limited introduction to the United

Version of Record, first published online February 20, 2019 with fixed content and layout in compliance with Art. 8.1.3.2 ICZN.

States and causing concern for future introductions of new strains of *R. lauricola* (Wuest et al. 2017).

Genetic variability within the native range of the vector beetle *X. glabratus* is unknown. Given that the species occurs in deciduous forests from southern Japan to northeastern India, genetic variation among populations is likely as high as observed for other Xyleborini species (Dole et al. 2010, Cognato et al. 2015, Gohli et al. 2017, Cognato et al. 2018). The sister species to *X. glabratus* and the diversity of related species are unknown; however, molecular phylogenies of Xyleborini suggest that a clade of globally distributed *Xyleborus* species is the closest related lineage (Cognato et al. 2011, 2018). The unusual elytral declivity morphology of *X. glabratus* also suggests that the species represents a monotypic clade.

As part of a multiyear survey of Southeast Asian Xyleborines, specimens of *X. glabratus* were collected from several locations in China, Taiwan, and Vietnam. We sequenced cytochrome oxidase I (COI), carbamoyl-phosphate synthetase 2, aspartate transcarbamylase, and dihydroorotase (CAD), and the large subunit ribosomal 28S DNA for a subset of these specimens in order to assess the genetic diversity within the beetle's native range. In the process, we discovered genetic variability among *X. glabratus* individuals and two lineages, which had a large amount of DNA sequence difference and associated morphological differences. These lineages are described here as new species.

Materials and Methods

Specimens

Eighteen specimens of *Xyleborus* species initially identified in the field as *X. glabratus* were included (Table 1). Specimens were excised from dead and dying tree parts or caught in ethanol-baited flight intercept traps. Prior to DNA extraction, a subset of specimens (one per morphospecies) was photographed with a Visionary Digital Passport II system (Palmyra, VA) using a Canon EOS 5D Mark II, 65.0 mm Canon Macro photo lens, Dynalite MH2015 road flash heads (Union, NJ), and a Stack Shot (Cognisys, Inc, Kingsley, MI). Montage images were created using Helicon Focus Mac Pro 6.7.1 (Helicon Soft, Kharkov, Ukraine). Specimens were examined using Leica (Wetzlar, Germany) MZ6 and MZ12.5 stereomicroscopes and illuminated with an Ikea Jansjö LED work lamp (Delft, the Netherlands). Final species identifications were made in reference to the lectotype specimen of *X. glabratus*, designated in this paper. Length was measured from the pronotum apex to the base of the elytral declivity. Pedicel is not included in the number of funicle segments, following Hulcr and Smith (2010).

The following entomological collections are referenced in the text:

IRSNB	Institut Royal des Sciences Naturelles de Belgique, Brussels, Belgium
IZAS	Institute of Zoology, Chinese Academy of Science, Beijing, China
MIZ	Zoological Museum, Museum and Institute of Zoology, Polish Academy of Science, Warsaw, Poland
MNHP	Museum of Natural History, Prague, Cechia
MSUC	A.J. Cook Arthropod Research Collection, Michigan State University, East Lansing, MI, United States
NHML	Natural History Museum, London, United Kingdom
NMNH	National Museum of Natural History, Smithsonian Institution, Washington DC, United States
NHMW	Naturhistorisches Museum Wien, Vienna, Austria
RABC	Roger A. Beaver collection, Chiang Mai, Thailand
UHZM	Universität Hamburg Zoological Museum, Hamburg, Germany
UFFE	Forest Entomology Lab, University of Florida, Gainesville, FL, United States

DNA Sequences

DNA was individually extracted from uncrushed prothoraces using a Qiagen DNEasy blood and tissue kit (Hilden, Germany) following the manufacturer's protocols. The intact prothoraces and the remaining body parts were vouchered in the MSUC. Aliquots of these purified DNA samples were used for the polymerase chain reaction (PCR) of COI, CAD, and 28S genes using general insect and scolytine-specific primers and protocols (Hebert et al. 2003, Smith and Cognato 2014). PCR products were produced using 17.25-µl ddH_2O, 2.5-µl 10× PCR buffer (Qiagen), 1.0-µl 25-mM $MgCl_2$ (Qiagen), 0.5-µl dNTP mix (Qiagen), 4.5-µl DNA template, 0.25-µl HotStar Taq DNA polymerase (Qiagen), and 0.75 µl of forward and reverse primers (COI: 1495b and rev750; CAD: apCADforB2 or apCADfor4 and apCADrev1mod; 28S: 3665 and 4068; see Smith and Cognato 2014 for details). PCRs were performed on a thermal cycler (PTC-2000, MJ Research, Waltham, MA, or MyCylcer Thermocycler, BioRad, Hercules, CA). PCR was performed under the following conditions: one cycle for 15 min at 95°C; 34 cycles for 30 s at 95°C, 30 s at 50°C (COI) or 55°C (CAD and 28S), 45 s at 72°C; and a final elongation cycle of 5 min at 72°C. PCR products were treated with Exo-SAP (USB Corp., Cleveland, OH) and sequenced in the Michigan State University Research Technology Support Facility using BigDye Terminator v1.1 (Applied Biosystems, Foster City, CA). Forward and reverse DNA strands were visualized in Sequencher (Ann Arbor, MI) to trim primer sequences, examine for ambiguities and create consensus sequences. Consensus sequences were blasted in GenBank to examine for potential contamination, pseudogenes, or both, none of which were found. Sequences were compiled as a Nexus file and deposited in GenBank (Table 1). The outgroup species *Xyleborus affinis* Eichhoff and *Xyleborus perforans* (Wollaston) were chosen because they represented closely related species to *X. glabratus* (Cognato et al. 2011). Their DNA sequences were retrieved from GenBank (Table 1).

Phylogenetic Analyses

Phylogenies were reconstructed PAUP*4.0 b10 PPC (Swofford 2002) using the criteria of parsimony and likelihood. For both analyses, heuristic searches with 100 stepwise random additions with tree bisection-reconnection were performed. Characters were unordered and equally weighted for the parsimony analysis. A GTR + I + G model for the likelihood analysis included six states with equal rates, empirical state frequencies, estimated invariable sites, and a gamma distribution for variable sites with shape = 0.5 (as in, Cognato et al. 2018). Bootstrap values under parsimony and likelihood criteria (under the same conditions above) were calculated by performing 500 pseudoreplicates with simple additions in PAUP*. Nucleotide difference among sequences was measured as uncorrected 'p' distance.

Species Concept

Species are hypotheses of evolutionary independent lineages (Hey 2006 and for example, Yeates et al. 2011). For this study, evidence for species includes the congruence between diagnostic morphological and molecular traits, monophyly, phylogenetic branches longer between clades than within clades, and/or nonoverlapping intra- and interspecific nucleotide differences.

Table 1. Specimens, labels, collection location, and GenBank numbers

Species	OTU label	Voucher code	Locality	GenBank	
				COI	CAD
Xyleborus affinis	N/A	Xylaff	Costa Rica	GU808696	GU808621
Xyleborus perforans	N/A	Xylperf	Papua New Guinea	HM064132	HM064311
Xyleborus glabratus	1	SAX 203	China: Hong Kong: New Territories	MK251515	MK251533
Xyleborus glabratus	2	SAX 239	China: Hong Kong: New Territories	MK251518	MK251536
Xyleborus glabratus	3	SAX 277	China: Hong Kong: New Territories, ex. *Machilus*	MK251519	MK251537
Xyleborus glabratus	4	SAX 278	China: Hong Kong: New Territories	MK251520	MK251538
Xyleborus glabratus	5	SAX 296	China: Hong Kong: New Territories	MK251521	MK251539
Xyleborus glabratus	6	SAX 202	China: Hong Kong: New Territories	MK251514	MK251532
Xyleborus glabratus	7	Xylgal20	Taiwan: Pinglin: Huisun Forest, ex. *Machilus* zuihoensis	MK251506	MK251524
Xyleborus glabratus	8	SAX 238	Taiwan: Pinglin: Chen Tea Farm	MK251517	MK251535
Xyleborus glabratus	9	Xylgal23	United States: Florida	MK251509	MK251527
Xyleborus glabratus	10	Xylgal19	United States: Louisana	MK251505	MK251523
Xyleborus glabratus	11	SAX 132	Vietnam: Cao Bang: Phia Oac Res.	MK251512	MK251530
Xyleborus glabratus	12	SAX 349	Vietnam: Ninh Binh: Cuc Phuong NP, ex. Lauraceae	MK251522	MK251540
Xyleborus glabratus	13	SAX 176	Vietnam: Thua Thien-Hue: Bach Ma NP, ex. Lauraceae	MK251513	MK251531
Xyleborus insidiosus	N/A	Xylgal22	Vietnam: Cao Bang: Phia Oac Res.	MK251508	MK251526
Xyleborus mysticulus	1	SAX 237	Taiwan: Pinglin: Chen Tea Farm, ex. *Machilus* sp.	MK251516	MK251534
Xyleborus mysticulus	2	Xylgal21	Vietnam: Cao Bang: Phia Oac Res.	MK251507	MK251525
Xyleborus mysticulus	3	Xylgal24	Vietnam: Cao Bang: Phia Oac Res.	MK251510	MK251528
Xyleborus mysticulus	4	Xylgal25	Vietnam: Cao Bang: Phia Oac Res.	MK251511	MK251529

N/A, not applicable.

Nomenclature

This paper and the nomenclatural act(s) it contains have been registered in Zoobank (www.zoobank.org), the official register of the International Commission on Zoological Nomenclature. The LSID (Life Science Identifier) number of the publication is as follows: urn:lsid:zoobank.org:pub:262B82F9-823C-4F93-8009-8546C28F5AC6

Results

In total, 1,266 nucleotides, 672 from COI, and 594 from CAD were included in the phylogenetic analyses. There was no nucleotide difference among the 28S sequences and these were excluded from the analyses. A longer region of CAD (~630 bp) that included a length variable intron (produced with PCR primers CADfor B2 and apCADrev1mod) was diagnostic for the three species (Fig. 1). This region was only sequenced for a subsample of individuals and therefore not included in the phylogenetic analysis. There were 164 and 25 parsimony-informative COI and CAD characters, respectively. Using the COI and CAD data together, the parsimony analysis found five most parsimonious trees and the likelihood analysis found four most likely trees. The strict consensus trees of the most parsimonious and the most likely trees were unresolved for *X. glabratus* from Hong Kong (Fig. 2). The placement of *X. mysticulus* n. sp. (Taiwan) sister to *X. insidiosus* n. sp. was the only difference between the parsimony (not shown) and likelihood tree (Fig. 2). Both analyses resolved a well-supported monophyletic *X. glabratus* including individuals from Hong Kong, Taiwan, Vietnam, and United States. Nine mtDNA haplotypes and four CAD genotypes were discovered—some with comparatively large nucleotide differences (Fig. 2). *Xyleborus mysticulus* n. sp. included a monophyletic group of individuals from Vietnam and Taiwan. Although this relationship was poorly supported, these individuals shared morphological characters diagnostic for *X. mysticulus*. One Vietnamese individual represented *X. insidiosus* n. sp. in the phylogeny as a long-branch sister to *X. glabratus* (Fig. 2). *Xyleborus insidiosus* n. sp. also occurs in China (Sichuan) as evidenced by museum specimens (see species description below).

Intra- and interspecific nucleotide differences for COI and CAD did not overlap among the species (Table 2). Considering all species, the intraspecific differences ranged from 0 to 0.1 and 0 to 0.013 and the interspecific differences ranged from 0.137 to 0.168 and 0.015 to 0.032 for COI and CAD, respectively. For *X. glabratus*, the DNA sequences from Vietnam (Thua Thien-Hue prov.) were the most different from conspecifics with means of 0.09 for COI and 0.007 for CAD. For some interspecific comparisons, the nucleotide difference was similar to comparisons made to the outgroup species (COI: 0.157–0.2, mean = 0.182; CAD: 0.03–0.052, mean = 0.045). In comparison to *X. glabratus*, the range of interspecific nucleotide differences for COI and CAD observed for *X. insidiosus* n. sp. and *X. mysticulus* n. sp. exceeded the maximum intraspecific differences for *X. glabratus* (Table 2).

The lineages labeled as *X. insidiosus* and *X. mysticulus* (Fig. 2) are described as new species, because they associate with diagnostic morphological and molecular characters and demonstrate nonoverlapping intra- and interspecific nucleotide differences. *Xyleborus glabratus* is redescribed to facilitate comparison to the new species, to present new distribution records, and to designate a lectotype. These three species represent a monophyletic group, which is diagnosed below so to facilitate identification compared with other *Xyleborus* species.

Xyleborus glabratus Eichhoff

(Figs. 3A–D and 4)

Xyleborus glabratus Eichhoff, 1877: 127. *Xyleborus kumamotoensis* Murayama, 1934: 288. syn. n.

Diagnosis: Small body size 2.20–2.50 mm long; anterior half of the pronotum strongly shining; discal interstriae two times

```
X. glabratus US: FL  CAGGAAATTCAGGAAAAAAAGAAG+AAAAAAATGTATGCCT
X. glabratus US: LA  CAGGAAATTCAGGAAAAAAAGAAGAAAAAAAATGTATGCCT
X. glabratus Taiwan CAGGAAATTCAGGAAAAAAAGAAGAAAAAAAATGTATGCCT
X. insidious        CAGGAAATTCAGG++++++++++AAAAAAAATGTATGCCT
X. mysticulus       CAGGAAATTCAGAA++++++++++AAAAAAAAT+TATGCCT
X. mysticulus       CAGGAAATTCAGAA++++++++++AAAAAAAAT+TATGCCT
X. mysticulus       CAGGAAATTCAGAA++++++++++AAAAAAAAT+TATGCCT
```

Fig. 1. Length variable region of a CAD intron: a potential species diagnostic character.

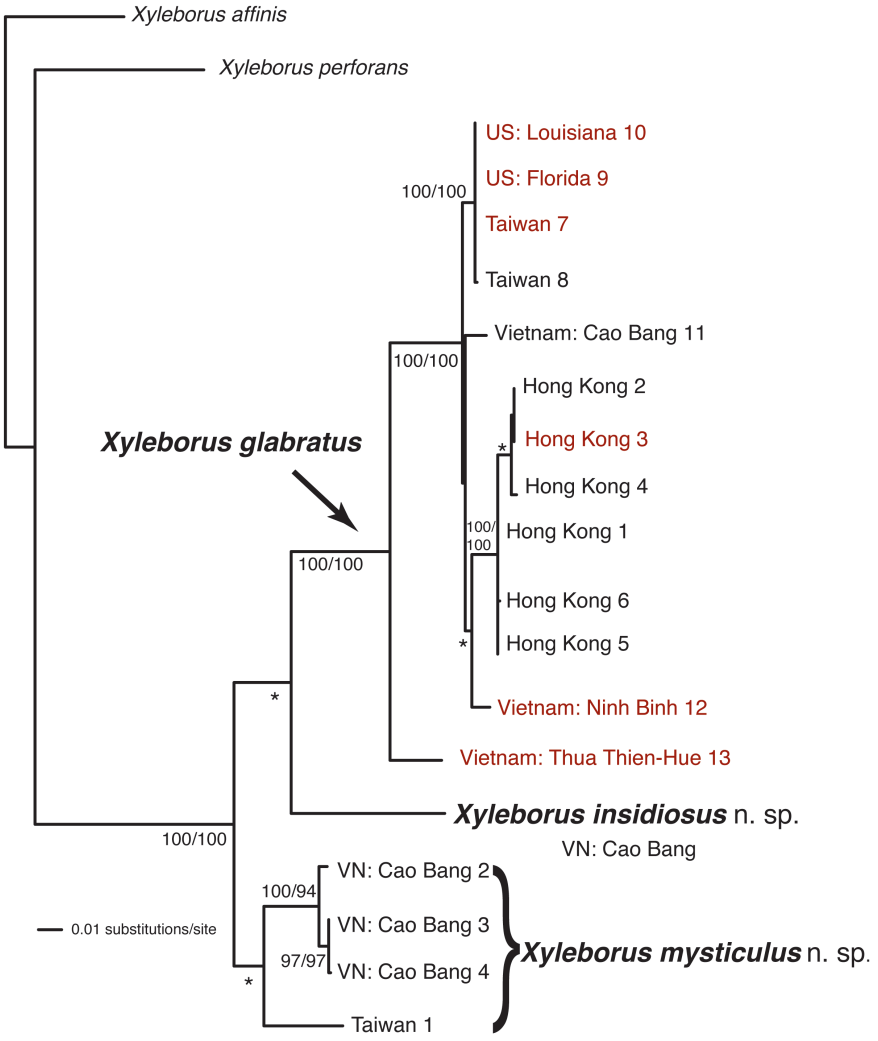

Fig. 2. One of four most likelihood trees found in a heuristic search using the COI and CAD data. The strict consensus of these trees was mostly resolved except for the relationships among some *X. glabratus* individuals. Five most parsimonious trees had a similar topology except for the placement of *X. mysticulus* from Taiwan. OTUs 3, 7, 9, 10, 12, & 13 = individuals collected from laurel trees exhibiting symptoms of disease. At nodes: #parsimony/#likelihood = bootstrap values and *bootstrap values < 70%.

the width of striae; discal strial punctures four to five times the diameter of those of interstriae; declivital striae and interstriae clearly distinguishable; declivital striae flat to feebly impressed; declivital interstriae denticulate and granulate, numerous closely spaced granules, and 1–3 small denticles (typically one), 1–3 larger denticles (typically three) on interstriae 1; and strongly developed posterolateral carina that extends from the apex to interstriae 7 (Figs. 3B and C and 4).

Redescription. Female. Length: 2.20–2.50 mm long (mean = 2.36 mm; n = 5); 3.14–3.57 times as long as wide. Body color uniformly ferrugineous to dark brown, but typically brown. Legs and antennae yellow-brown. Appearing glabrous with sparse setae on the anterior third of the pronotum.

Head. Epistoma entire, transverse, lined with a row of long hair-like setae. Frons feebly to weakly convex from epistoma to upper level of eyes with a weak median carina extending from

Table 2. Average and range of pairwise uncorrected 'p' differences

	Lower diagonal COI	Upper diagonal CAD	
Interspecific	*Xyleborus glabratus*	*Xyleborus insidious*	*Xyleborus mysticulus*
Xyleborus glabratus	+	0.024 (0.021–0.032)	0.017 (0.015–0.024)
Xyleborus insidious	0.168 (0.137–0.168)	+	0.015 (n/a)
Xyleborus mysticulus	0.16 (0.143–0.16.8)	0.144 (0.143–0.145)	+
Intraspecific			
	COI	CAD	
Xyleborus glabratus	0.034 (0–0.10)	0.003 (0–0.013)	
Xyleborus insidious	n/a	n/a	
Xyleborus mysticulus	0.01	0	
Compared to outgroups			
	0.182 (0.157–0.2)	0.45 (0.03–0.052)	

epistoma to upper level of eyes; surface shagreened, dull, punctate; punctures uniformly sized, sparse; sparse erect hair-like vestiture in lateral areas. Eyes deeply emarginated above level of antennal insertion, upper portion of eyes smaller than lower part. Submentum flat, deeply impressed below genae, very narrow, triangular. Scape regularly thick, about as long as length of club. Antennal funicle four segmented, segments equal in size. Pedicle as long as funicle. Club 1.6 times taller than broad, asymmetrical; club type 2 (Hulcr et al. 2007), obliquely truncate; segment 2 visible on posterior face, appearing soft, segment 1 covering most of posterior face, its margin completely costate; segment 1 on anterior face corneous, occupying approximately basal 40% (37–42%); segment 2 narrow, pubescent with corneous part visible on anterior face only.

Pronotum. 1.3 times as long as wide. Sides straight; pronotum elongated, with low summit from lateral view (type 7, Hulcr et al. 2007). Anterior margin basic, parallel-sided, rounded when viewed dorsally (type 2, Hulcr et al. 2007), lacking a row of serrations. Surface strongly shining, anterior half finely asperate, asperities close, arranged in concentric rings from midpoint of pronotum to anterior margin; each asperity bearing a single semi-erect hair-like seta; disc glabrous, feebly and sparsely punctate. Lateral margins rounded. Base straight.

Legs. Procoxae contiguous, prosternal posterocoxal piece large, inflated. Protibia obliquely triangular, broadest at apical third, posterior face flat, unarmed; three to five small socketed denticles present on outer margin of apical third. Mesotibia strongly flattened, obliquely triangular, broadest at apical third; posterior face flat, unarmed; six small socketed denticles present on apical third. Metatibia with evenly rounded outer margin, flattened, posterior face unarmed, six to seven socketed denticles present on outer margin.

Elytra. Elytral base transverse, humeral angles rounded. Scutellum moderately sized, 'u' shaped, flat, flush with elytra. Sides straight from base to apical half of declivity; lateral profile of declivity steep, convex; apex entire, rounded. Disc occupying two-third of total elytral length. Disc smooth, shining, glabrous; strial and interstrial punctures uniseriate, parallel; interstriae two times as wide as striae, minutely, sparsely punctate; striae not impressed; punctures irregularly spaced, four to five times the diameter of those of interstriae. Declivital face shining; declivital interstriae 1 laterally broadened from base to declivital midpoint and then narrowing toward apex; strial punctures coarse, denser, larger than on disc, approximately equal sized; interstriae impunctate; striae and interstriae clearly distinguishable; interstriae variously denticulate and granulate (often asymmetric, see Remarks); interstriae 1 with at least one large denticle (typically 3) and numerous closely spaced granules and one to three small denticles (typically 1); remaining interstriae with numerous smaller denticles and granules; denticles bearing a short, semi-erect seta at base; striae flat to feebly impressed. Posterolateral declivital costa strongly developed, extending from apex to interstriae 7.

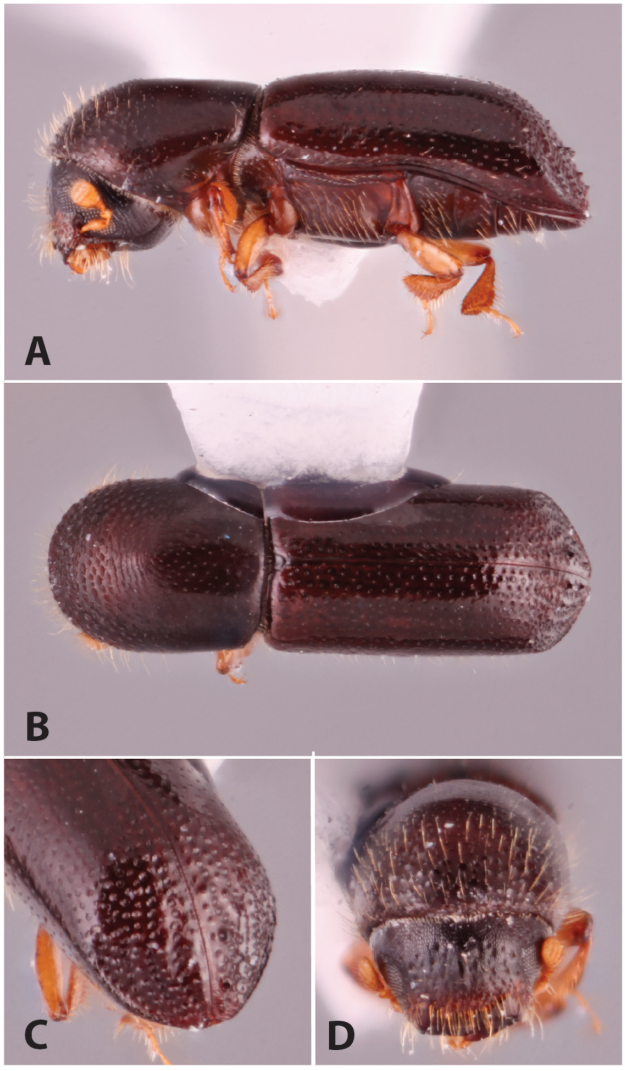

Fig. 3. *Xyleborus glabratus.* Female habitus: **(A)** lateral; **(B)** dorsal; **(C)** posterior oblique; **(D)** frontal.

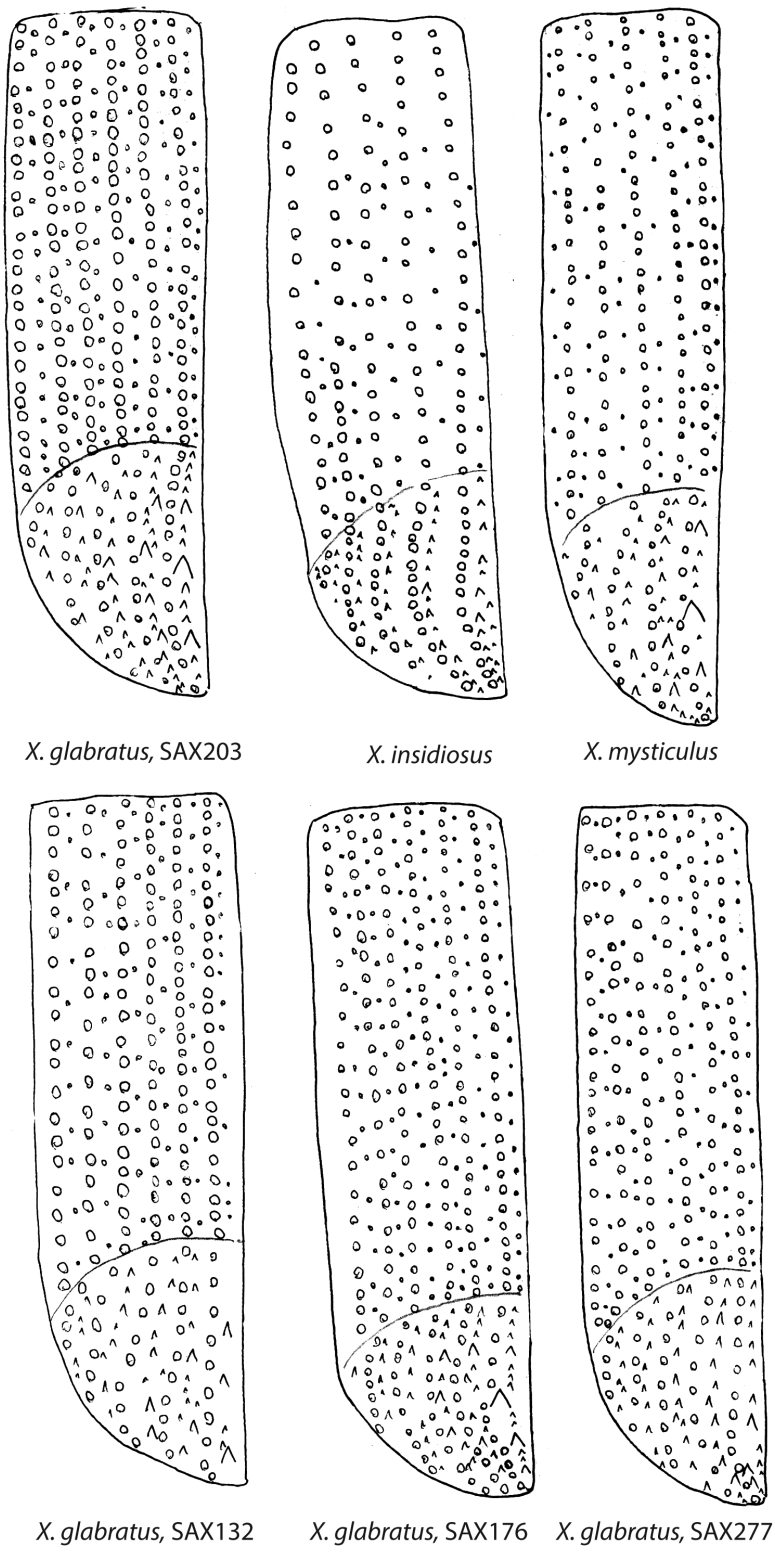

Fig. 4. Sketches of the left elytron (at 125× magnification) for *X. glabratus, X. insidiosus* and *X. mysticulus*. Sketches emphasize the arrangement and size of granules (∧) and punctures (o). Setae and tumescences are not shown. *Xyleborus glabratus* (SAX203) was compared to the lectotype and has similar morphology. Other illustrations of *X. glabratus* show typical variation of granules and punctures.

Distribution: Bangladesh, China (Fujian, Guangdong, Guangxi, Hunan, Jiangxi, Sichuan), India (Assam, Bengal), Japan, Myanmar, Taiwan, Thailand, and Vietnam. Imported to and established in United States (Wood and Bright 1992, Beaver et al. 2014, Smith et al. 2018b).

New records: CHINA: Guangxi, Malu, 27.iii.2018, You Li, ex. *Cinnomommon cassia* (UFFE, 1). Guangdong, Danxia Shan NP, Wo Long Gang Forest Walkway, 25°01.3′N, 113°44.5′E, 100 m, 23–26.iv.2013, J. Háyek & J.T. Růžička (RABC, 1). Hong Kong,

New Territories, 1.vi.2017, J. Hulcr, Y. Li, J. Skelton, P. Carlson, B. Guenard & B. Hau (UFFE, 6). Jiangxi, Jinggang Shan Mts., Xiangzhu vill. env., 26°35.5′N, 114°16.0′E, 374 m, rice fields, forested stream valley, M. Fikáček, J. Hájek (MNHP, 1); as previous except: Jinggang Mt., 21.v.2017, Lai-S-C. (RABC, 1). TAIWAN: Huisun Forest, 10.iv.2015, ex. recollection from the same tree with squirrel damage/wilt symptoms orig. found iii.2015, A. Black & J. Skelton, ex. *Machilus zuihoensis* (NMNH, 1). VIETNAM: Cao Bang prov., 22°36.804′N 105°51.982′E, 1831 m, 17.iv.2014, VN43, Cognato, Smith, Pham, ex. punky log (MSUC, 5). Ninh Binh prov., Cuc Phuong N.P., 7.iii.2018, 20.34932, 105.59669, 431 m, A.I. Cognato & S.M. Smith, ex. standing dead Lauraceae, 5 cm at base (MSUC, 9). Quang Tri prov., Huong Hoa district, Huong Hoa Nature Reserve, near Cup village, 16°56′15N, 106°34′52E, 400 m, 6.xi.2007, G. Csorba (RABC, 1). Thua Thien-Hue prov., Bach Ma NP, 16.19734, 107.8551, 1356 m, 17–18.ii.2017, VN73, AI Cognato, TA Hoang, ex. standing laurel 12 cm dia (MSUC, 6).

Host plants: The species has an evident preference for the family Lauraceae, and its attacks are restricted to that family in the United States (Rabaglia et al. 2006, Fraedrich et al. 2008). In the Oriental region it has also been recorded on a few occasions from different families including Dipterocarpaceae, Fabaceae, Fagaceae, Pinaceae, and Theaceae (Beaver and Liu 2010, Hulcr and Lou 2013), but it is unclear whether individuals were breeding in these trees.

Remarks: The elytral declivity is variable among individuals and often between each elytron of a single individual (Fig. 4). In general, declivital interstriae 1 typically has three large denticles and a single additional small denticle. However, individual elytra may have one to three large and one to three small denticles on interstriae 1. The number of denticles of any size can vary significantly on the other declivital interstriae, especially interstriae 2 and 3. Each of these interstriae exhibits a range of zero to three denticles, which can vary among individuals collected from the same tree. However, we generally observed four main varieties of elytral declivital granulation (Fig. 4).

Xyleborus glabratus was described from an unspecified number of specimens (Eichhoff 1877). Eichhoff's collection and types were deposited in UZHM (Hamburg, Germany) and were destroyed when the museum was bombed during WWII. Approximately a dozen Eichhoff types were saved by K.E. Schedl as detailed by Wood and Bright (1992). These types are deposited in Schedl's collection in NHMW and only two Eichhoff type specimens remain in the Hamburg collection (Weidner 1976). Wood and Bright (1992) list the syntype series as deposited in IRSNB. However, type specimens of *X. glabratus* are not present in this collection (Pol Limbourg, pers. comm, 31.vii.2017). Specimens are also not present in NHMW (Schedl 1979). A single remaining syntype was located in MIZ. A similar erroneous IRSNB depository was also listed for *Xyleborus festivus* Eichhoff (Wood and Bright 1992), the holotype of which is still present in UHZM as detailed in Smith et al. (2018a).

To ensure correct and consistent application of the name, we here designate the female specimen from Japan as the lectotype of *Xyleborus glabratus* Eichhoff. The lectotype is labeled "Japan Hiller [typed] \ coll. Kraatz Hagedorn det. [typed] \ *Xyleborus glabratus* ♀ & ♂ [handwritten] \ Dtsch. Entomol. Institut Berlin [typed]\ ex. coll. M. Nunberg Inst. Zool. PHN Warsawa 28/79 [handwritten] \ [red label] Mus. Zool. Polonicum Warszawa Typus 784 *Xyleborus glabratus* Eichhoff 1877 SYNTYPUS \ [red label] LECTOTYPE *Xyleborus glabratus* Eichhoff [typed]'. The specimen is the last remaining Eichhoff syntype and is deposited in MIZ. The male specimen referred to on the label is missing.

The lectotype of *X. glabratus* (Hagi, Kagoshima Prefecture, Chugoku region, Honshu) (MIZ) and the female syntype of *X. kumamotoensis* (Jissa, Yagamuchi Prefecture, Kyushu) (NMNH) were directly compared. Though collected from different islands, both specimens were collected within relatively close geographic area. The morphology of the two specimens was found to be conspecific and *X. kumamotoensis* is here placed in synonymy.

Xyleborus insidiosus Cognato & Smith n. sp.

(Figs. 4 and 5A–D)

(Zoobank LSID: urn:lsid:zoobank.org:act:1104F78F-A89C-49A9-93E4-B078F7F65612)

Diagnosis: Large body size, 2.70–2.80 mm long; anterior half of pronotum distinctly shagreened; broad discal interstriae, four times the width of discal striae; discal strial punctures three times the diameter of those of interstriae; declivital striae and interstriae clearly distinguishable; declivital striae clearly impressed; interstriae uniformly granulate, never denticulate; and strongly developed posterolateral carina that extends from the apex to interstriae 6 (Figs. 4 and 5B and C).

Type material: Holotype, female: Vietnam: Cao Bang prov., 22°36.804′N 105°51.982′E, 1831 m, 17.iv.2014, VN43, Cognato, Smith, Pham, ex. punky log (MSUC). Paratypes, female: as holotype except: VN46, ex. punky bark (MSUC, 4; NHML, 1); CHINA: Sichuan, Leibo, 800 m, 16.iv.1964, Fusheng Huang, ex. Fagaceae (IZAS, 1; NMNH, 3).

Description: Female. 2.70–2.80 mm long (mean = 2.74 mm; n = 5); 3.00–3.50 times as long as wide. Body and legs uniformly dark brown. Appearing glabrous with sparse setae on the anterior third of the pronotum.

Head. Epistoma entire, transverse, lined with a row of long hair-like setae. Frons feebly to weakly convex from epistoma to upper level of eyes with a weak median carina extending from epistoma to upper level of eyes; surface shagreened, dull, punctate; punctures uniformly sized, sparse; sparse erect hair-like vestiture in distributed evenly across frons. Eyes deeply emarginated above level of antennal insertion, upper portion of eyes smaller than lower part. Submentum flat, deeply impressed below genae, very narrow, triangular. Scape regularly thick, about as long as length of club. Antennal funicle four segmented, segments equal in size. Pedicle as long as funicle. Club 1.6 times taller than broad, asymmetrical; club type 2 (Hulcr et al. 2007), obliquely truncate, segment 2 visible on posterior face, appearing soft; segment 1 on anterior face corneous, covering most of posterior face, its margin completely costate; segment 1 corneous, occupying approximately basal 40% of club; segment 2 narrow, pubescent with corneous part visible on anterior face only.

Pronotum. 1.1–1.2 times as long as wide. Sides straight; pronotum elongated, with low summit from lateral view (type 7, Hulcr et al. 2007). Anterior margin basic, parallel-sided, rounded when viewed dorsally (type 2, Hulcr et al. 2007), lacking a row of serrations. Basal half strongly shining, anterior half strongly shagreened,

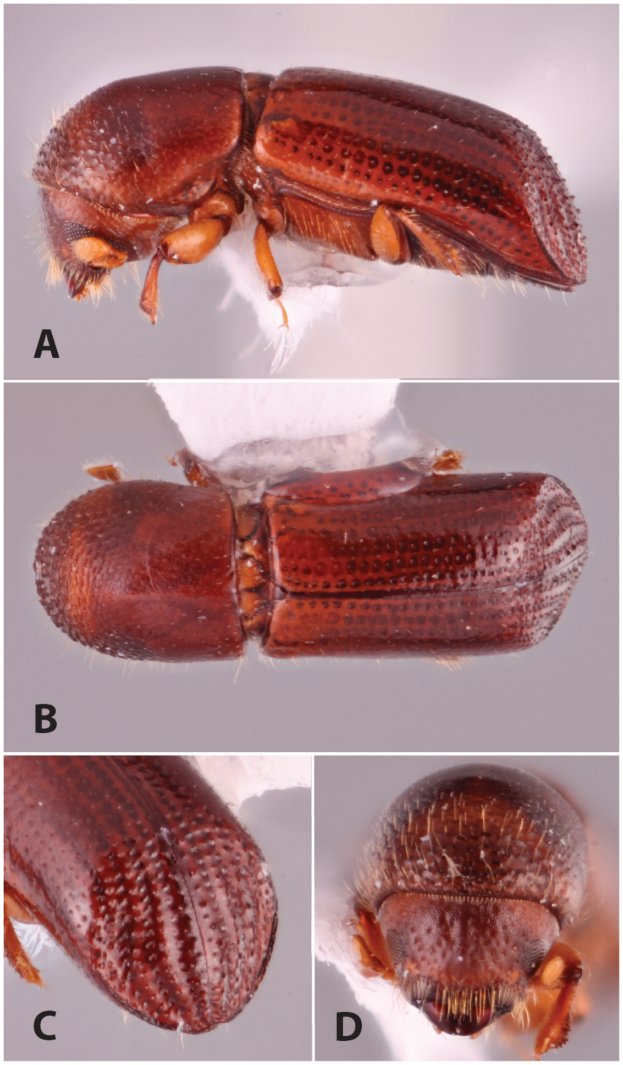

Fig. 5. *Xyleborus insidiosus*. Holotype, female habitus: **(A)** lateral; **(B)** dorsal; **(C)** posterior oblique; and **(D)** frontal.

anterior half finely asperate, asperities close, arranged in concentric rings from midpoint of pronotum to anterior margin; each asperity bearing a single semi-erect hair-like seta; disc glabrous, feebly and sparsely punctate. Lateral margins rounded. Base straight.

Legs. Procoxae contiguous, prosternal posterocoxal piece large, inflated. Protibia obliquely triangular, broadest at apical third, posterior face flat, unarmed; four to five small socketed denticles present on outer margin of apical third. Mesotibia strongly flattened, obliquely triangular, broadest at apical third; posterior face flat, unarmed; four to six small socketed denticles present on apical third. Metatibia with evenly rounded outer margin, flattened; posterior face unarmed, six socketed denticles present on outer margin.

Elytra. Elytral base transverse, humeral angles rounded. Scutellum moderately sized, 'u' shaped, flat, flush with elytra. Sides straight from base to apical half of declivity; lateral profile of declivity steep, convex; apex entire, rounded. Disc occupying two-third of total elytral length. Disc smooth, shining; strial and interstrial punctures uniseriate, parallel; interstriae four times as wide as striae, minutely, sparsely punctate, each puncture bearing a short semi-erect hair-like seta; striae not impressed; punctures irregularly spaced, three times the diameter of those of interstriae. Declivital face shining; declivital interstria 1 laterally broadened from base to declivital midpoint and then narrowing toward apex; strial punctures denser, larger than on disc; striae and interstriae clearly distinguishable; interstriae impunctate; granules uniformly sized on each interstriae, decreasing in size laterally from interstria 1, granules bearing a short semi-erect hair-like seta at its base. Striae clearly, distinctly impressed. Posterolateral declivital costa strongly developed, extending from apex to interstriae 6.

Etymology: *insidiosus* = (L.) cunning, deceitful.

Distribution: China (Sichuan), Vietnam.

Host plants: This species has been collected from Fagaceae as well as unidentified punky wood.

Remarks: Specimens of *Xylebrous insidiosus* were collected together with *X. glabratus* at both collection events in Vietnam (VN43 and VN46).

Xyleborus mysticulus Cognato & Smith n. sp.

(Figs. 4 and 6A–D)

(Zoobank LSID: urn:lsid:zoobank.org:act: CE6DF2CB-767E-4ECB-BAAA-9E5B0A0315BB)

Diagnosis: Small body size 2.20–2.50 mm long; anterior half of pronotum strongly shining; discal interstriae that are two times the width of discal striae; discal strial punctures three times larger than interstrial punctures; declivital striae and interstriae difficult to distinguish; declivital striae not impressed; declivital interstriae denticulate and granulate, denticles on low tumescences giving the declivity a rugged sculptured appearance, one to three larger denticles on interstriae 1; and strongly developed posterolateral carina that extends from the apex to interstriae 7 (Figs. 4 and 6B and C).

Type material: Holotype, female: VIETNAM: Cao Bang prov., 22°36.454′N 105°52.083′E, 1661 m, 15.iv.2014, VN37, Cognato, Smith, Pham, ex. standing dead ~25 cm DBH tree (MSUC). Paratypes, female: same locality as holotype (MSUC, 8; NMNH, 2; NHML, 2); TAIWAN: Pinglin, Chen tea farm, 16.ix.2015, ex. fallen branch with other beetle spp., A. Black & J. Skelton, ex. *Machilus* sp. (MSUC, 1).

Description: Female. Length: 2.20–2.50 mm long (mean = 2.38 mm; n = 5); 3.14–3.57 times as long as wide. Body color uniformly ferrugineous to dark brown. Legs and antennae yellow-brown. Appearing glabrous with sparse setae on the anterior third of the pronotum.

Head. Epistoma entire, transverse, lined with a row of long hair-like setae. Frons feebly to weakly convex from epistoma to upper level of eyes with a weak median carina extending from epistoma to upper level of eyes; surface shagreened, dull, punctate; punctures uniformly sized, sparse; sparse erect hair-like vestiture in distributed evenly across frons. Eyes deeply emarginated above level of antennal insertion, upper portion of eyes smaller than lower part. Submentum flat, deeply impressed below genae, very narrow, triangular. Scape regularly thick, about as long as

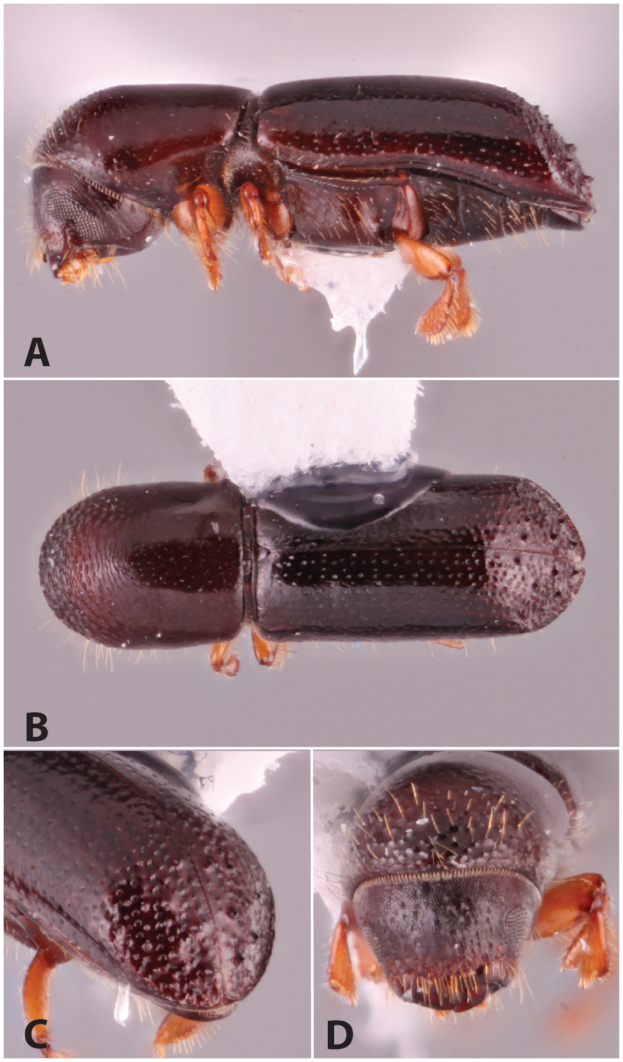

Fig. 6. *Xyleborus mysticulus*. Holotype, female habitus: **(A)** lateral; **(B)** dorsal; **(C)** posterior oblique; **(D)** frontal.

length of club. Antennal funicle four segmented, segments equal in size. Pedicle as long as funicle. Club 1.3 times taller than broad, symmetrical; club type 2 (Hulcr et al. 2007), obliquely truncate, segment 2 visible on posterior face, appearing soft; segment 1 covering most of posterior face, its margin completely costate; segment 1 on anterior face corneous, occupying approximately basal 40% of club; segment 2 narrow, pubescent with corneous part visible on anterior face only.

Pronotum. 1.1–1.2 times as long as wide. Sides straight; pronotum elongated, with low summit from lateral view (type 7, Hulcr et al. 2007). Anterior margin basic, parallel-sided, rounded when viewed dorsally (type 2, Hulcr et al. 2007), lacking a row of serrations. Basal half strongly shining, anterior half strongly shagreened, finely asperate, asperities close, arranged in concentric rings from midpoint of pronotum to anterior margin; each asperity bearing a single semi-erect hair-like seta; disc glabrous, feebly and sparsely punctate. Lateral margins rounded. Base straight.

Legs. Procoxae contiguous, prosternal posterocoxal piece large, inflated. Protibia obliquely triangular, broadest at apical third, posterior face flat, unarmed; three small socketed denticles present on outer margin of apical third. Mesotibia strongly flattened, obliquely triangular, broadest at apical third; posterior face flat, unarmed; five small socketed denticles present on apical third. Metatibia with evenly rounded outer margin, flattened; posterior face unarmed, six socketed denticles present on outer margin.

Elytra. Elytral base transverse, humeral angles rounded. Scutellum moderately sized, 'u' shaped, flat, flush with elytra. Sides straight from base to apical half of declivity; lateral profile of declivity steep, convex; apex entire, rounded. Disc occupying two-third of total elytral length. Disc smooth, shining, glabrous; strial and interstrial punctures uniseriate, parallel; interstriae twice as wide as striae, minutely, sparsely punctate; striae not impressed; punctures irregularly spaced, three times the diameter of those of interstriae. Declivital face shining, largely glabrous; declivital interstriae 1 laterally broadened from base to declivital midpoint and then narrowing toward apex; strial and punctures coarse, denser, larger than on disc; interstriae impunctate; striae and interstriae difficult to distinguish; interstriae asymmetric, variously denticulate and granulate; denticles on low tumescences giving the declivity a rugged sculptured appearance, each denticle bearing a short, semi-erect seta at the base; interstriae 1 with one to two large denticles and one to two small denticles; remaining interstriae with numerous smaller denticles; striae flat. Posterolateral declivital costa strongly developed, extending from apex to interstriae 7.

Etymology: *mysticulus* = (L.) secret (diminutive).

Distribution: Taiwan, Vietnam.

Host plants: *Machilus* sp. (Lauraceae).

Remarks: Although the clade that includes *X. mysticulus* is not well-supported, the species diagnostic characters of this specimen are indistinguishable from the diagnostic characters of the other *X. mysticulus* specimens.

Xyleborus glabratus species group

Included species: *Xyleborus glabratus* Eichhoff, *X. insidiosus* Cognato & Smith n. sp., and *X. mysticulus* Cognato & Smith n. sp.

Diagnosis: These species are distinguished from other *Xyleborus* species by declivital interstriae 1 laterally broadened from base to declivital midpoint and narrowing toward apex.

Phylogenetic placement: These species form a monophyletic group related to globally distributed *Xyleborus* species (e.g., *X. affinis, X. perforans*) in the context of a 150 xyleborine species phylogeny based on COI and CAD data (Cognato, unpublished). More data-rich phylogenetic analyses including only *Xyleborus glabratus* support the above observation and also suggest a close relationship to a clade of endemic Hawaiian *Xyleborus* spp (Cognato et al. 2011, 2018).

Discussion

DNA sequence data from COI and CAD genes representing widely dispersed populations of *X. glabratus* demonstrated multiple genotypes, some of which are associated with isolated localities (Table 1). Region-specific genotypes with gradual overlap is a typical pattern for bark and ambrosia beetles (e.g., Cognato et al. 1999, Storer et al. 2017), although isolation by distance has a greater effect on the fixation of genetic differences for the highly inbred xyleborines

(e.g., Cognato and Sun 2007, Jordal and Kambestad 2014, Cognato et al. 2015). 28S sequence differences were not observed, although population level differences have been observed for *Xylosandrus* species (Dole et al. 2010). Phylogenetic resolution based on 28S data is most predictable among genera and deeply divergent xyleborine species (Jordal et al. 2008, Dole et al. 2010, Jordal and Kambestad 2014, Stouthamer et al. 2017).

Intra- and interspecific nucleotide differences for COI and CAD are similar to those observed in previous xyleborine studies (Dole et al. 2010, Jordal and Kambestad 2014, Stouthamer et al. 2017). *Xylosandrus* species demonstrated 0.3–10% COI and 0.1 –0.8% CAD intraspecific nucleotide differences (Dole et al. 2010). However, 12–16% COI intraspecific nucleotide differences associated with paraphyletic lineages of *Xyleborinus saxsenii* (Ratzeburg) and clades of *Euwallaca fornicatus* (Eichhoff) (Jordal and Kambestad 2014, Stouthamer et al. 2017). Four species were recently recognized within the *E. fornicatus* complex (Gomez et al. 2018), but taxonomic actions have yet to be taken for *X. saxesenii*.

Our assessment of the new species described here is concordant with these previous observations and with an emerging pattern of COI and CAD intraspecific nucleotide differences based on a larger DNA taxonomic study of xyleborine species (>400 individuals representing 150 species). Intraspecific COI and CAD differences nearing 10 and 2%, respectively, suggest the potential for undescribed species (Cognato, unpublished). When associated with morphological (or biological) differences, these divergent lineages may be recognized as new species, as in *X. insidiosus* and *X. mysticulus*. Conversely, the lineage of *X. glabratus* from Thua Thien-Hue, Vietnam was not described as new even though it exhibited 9% COI intraspecific difference (Table 2, Fig. 2). Diagnostic characters were not found that differentiated this lineage from the remaining *X. glabratus* (Fig. 4, SAX176).

As reported here, recent scolytine-targeted collecting in Southeast Asia yielded multiple specimens of *X. glabratus* and extended its known range further south to 16° latitude (Thua Thien-Hue, Vietnam). It is likely that *X. glabratus* occurs throughout the range of its laurel hosts which includes much of eastern and southern Asia. Potentially, *X. glabratus* may occur as far north as 40° latitude (near Beijing, China) as suggested by cold tolerance experiments (Formby et al. 2018). *Xyleborus insidiosus* and *X. mysticulus* were collected at higher elevations and maybe restricted to the cooler habitats of cloud forests.

This study provides additional records of the association of *X. glabratus* with laurel trees exhibiting symptoms of laurel wilt within the beetle's native range (Table 1, Fig. 2). *Raffaelea lauricola* cultured from symptomatic laurel tree provided direct evidence for the association between the Taiwanese *X. glabratus* and laurel wilt (Hulcr et al. 2017), whereas only leaf flagging and branch dieback was associated with the Vietnamese *X. glabratus* individuals (Fig. 2). Specimens from Hong Kong were collected from recently dead and apparently diseased lauraceous hosts, but the role of *X. glabratus* in this mortality was unclear. These beetles exhibited various degrees of relatedness from sharing the same mtDNA COI haplotype to exhibiting a p-distance value of 0.09. A relatively similar range of p-distances was observed for CAD. These results suggest that these beetle lineages may associate with phenotypes suited for different climates given they were collected at different latitudes. Different laurel wilt fungal strains, as recorded from the native range (Wuest et al. 2017), may also associate with the beetle lineages and these fungal strains may exhibit various degrees of pathogenicity, as observed for other fungi (for example, O'Donnell et al. 1998). More detailed research of the beetle lineages' adaptation to different climates and of the association among fungal strains and beetle lineages is needed. In the absence of further knowledge at this time, it is prudent to remain vigilant of the potential spread of these beetle lineages beyond their native range. If these additional beetle lineages from the southern extent of their range can tolerate hotter and drier conditions, then the more arid areas of California and Mexico may be at greater risk of infestation by yet-introduced *X. glabratus* lineages and laurel wilt, which places a greater risk onto the loss of the world's largest avocado industry (Lira-Noriega et al. 2018).

Acknowledgments

We thank Gina Sari (MSU) for help generating DNA sequences, Jun Kai Wang for the illustrations and Tuan Anh Hoang (VNMN) for field assistance. Dr. Roger Beaver kindly added previously unpublished locality records. Additional thanks to Dr. Billy Hau and Dr. Benoit Guénard from the Hong Kong University and to Hong Kong Agriculture, Fisheries and Conservation Department for supporting the field collection. This study was funded by USDA-APHIS Cooperative Agreement Award 16-8130-0666-CA to A. I. C., and, in part, by grants from the USDA-APHIS Farm Bill section 10007, the USDA Forest Service, the National Science Foundation, and the Florida Forest Service to J. H.

References Cited

Beaver, R. A., and L. -Y. Liu. 2010. An annotated synopsis of Taiwanese bark and ambrosia beetles, with new synonymy, new combinations and new records (Coleoptera: Curculionidae: Scolytinae). Zootaxa 2602: 1–47.

Beaver, R. A., W. Sittichaya, and L. Y. Liu. 2014. A synopsis of the scolytine ambrosia beetles of Thailand (Coleoptera: Curculionidae: Scolytinae). Zootaxa. 3875: 1–82.

Cognato, A. I., and J. H. Sun. 2007. DNA based cladograms augment the discovery of a new *Ips* species from China (Coleoptera: Curculionidae: Scolytinae). Cladistics 23: 539–551.

Cognato, A. I., S. J. Seybold, and F. A. H. Sperling. 1999. Incomplete barriers to mitochondrial gene flow between pheromone races of the North American pine engraver, *Ips pini* (Say). Proc. R. Soc. B. 266: 1843–1850.

Cognato, A. I., J. Hulcr, S. A. Dole, and B. H. Jordal. 2011. Phylogeny of haplo-diploid, fungus-growing ambrosia beetles (Curculionidae: Scolytinae: Xyleborini) inferred from molecular and morphological data. Zool. Scr. 4: 174–186.

Cognato, A. I., E. R. Hoebeke, H. Kajimura, and S. M. Smith. 2015. History of the Exotic Ambrosia Beetles *Euwallacea interjectus* and *Euwallacea validus* (Coleoptera: Curculionidae: Xyleborini) in the United States. J. Econ. Entomol. 108: 1129–1135.

Cognato, A. I., B. H. Jordal, and D. Rubinoff. 2018. Ancient "wanderlust" leads to diversification of endemic Hawaiian *Xyleborus* species (Coleoptera: Curculionidae: Scolytinae). Insect System. Divers. 2: 1.

Dole, S. A., B. H. Jordal, and A. I. Cognato. 2010. Polyphyly of *Xylosandrus Reitter* inferred from nuclear and mitochondrial genes (Coleoptera: Curculionidae: Scolytinae). Mol. Phylogenet. Evol. 54: 773–782.

Eichhoff, W. J. 1877. Japanische Scolytidae. Dtsch. Entomol. Z. 21: 117–128.

Fraedrich, S. W., T. C. Harrington, R. J. Rabaglia, M. D. Ulyshen, A. E. Mayfield, J. L. Hanula, J. M. Eickwort, and D. R. Miller. 2008. A fungal symbiont of the redbay ambrosia beetle causes a lethal wilt in redbay and other Lauraceae in the southeastern United States. Plant Dis. 92: 215–224.

Formby, J. P., J. C. Rodgers III, F. H. Koch, N. Krishnan, D. A. Duerr, and J. J. Riggins. 2018. Cold tolerance strategy and invasive potential of the redbay ambrosia beetle (*Xyleborus glabratus*) in the eastern United States. Biol. Invasions 20: 995–1007.

Gohli, J., T. Selvarajah, L. R. Kirkendall, and B. H. Jordal. 2017. Globally distributed *Xyleborus* species reveal recurrent intercontinental dispersal in a landscape of ancient worldwide distributions. BMC Evol. Biol. 16: 37.

Gomez, D.F., J. Skelton, M.S. Steininger, R. Stouthamer, P. Rugman-Jones, W. Sittichaya, R. J. Rabaglia, and J. Hulcr. 2018. Species delineation

within the *Euwallacea fornicatus* complex revealed by morphometric and phylogenetic analyses. Insect Syst. Diver. 2(6): 1–11.

Hebert, P. D., A. Cywinska, S. L. Ball, and J. R. deWaard. 2003. Biological identifications through DNA barcodes. Proc. Biol. Sci. 270: 313–321.

Hey, J. 2006. On the failure of modern species concepts. Trends Ecol. Evol. 21: 447–450.

Hughes, M. A., J. J. Riggins, F. H. Koch, A. I. Cognato, C. Anderson, J. P. Formby, T. J. Dreaden, R. C. Ploetz, and J. A. Smith. 2017. No rest for the laurels: symbiotic invaders cause unprecedented damage to southern USA forests. Biol. Invasions 19: 2143–2157.

Hulcr, J., and Q. Z. Lou. 2013. The redbay ambrosia beetle (Coleoptera: Curculionidae) prefers Lauraceae in its native range: records from the Chinese National Insect Collection. Fla. Entomol. 96: 1595–1596.

Hulcr, J., and S. M. Smith. 2010. Xyleborini ambrosia beetles: an identification tool to the world genera. Available at: http://itp.lucidcentral.org/id/wbb/xyleborini/index.htm (accessed 10 September 2018).

Hulcr, J., S. A. Dole, R. A. Beaver, and A. I. Cognato. 2007. Cladistic review of generic taxonomic characters in *Xyleborina* (Coleoptera: Curculionidae: Scolytinae). Syst. Entomol. 32: 568–584.

Hulcr, J., A. Black, K. Prior, C.-Y. Chen, and H. -F. Li. 2017. Studies of ambrosia beetles (Coleoptera: Curculionidae) in their native ranges help predict invasion impact. Fla. Entomol. 100: 257–261.

Jordal, B. H., and M. Kambestad. 2014. DNA barcoding of bark and ambrosia beetles reveals excessive NUMTs and consistent east-west divergence across Palearctic forests. Mol. Ecol. Resour. 14: 7–17.

Jordal, B., J. J. Gillespie, and A. I. Cognato. 2008. Secondary structure alignment and direct optimization of 28SrDNA sequences provide limited phylogenetic resolution in bark and ambrosia beetles (Curculionidae: Scolytinae). Zoologica Scripta 37: 43–56.

Kendra, P. E., W. S. Montgomery, J. Niogret, and N. D. Epsky. 2013. An uncertain future for American Lauraceae: a lethal threat from redbay ambrosia beetle and laurel wilt disease (a review). Am. J. Plant Sci. 4: 727–738.

Lira-Noriega, A., J. Soberón, and J. Equihua. 2018. Potential invasion of exotic ambrosia beetles *Xyleborus glabratus* and *Euwallacea* sp. in Mexico: a major threat for native and cultivated forest ecosystems. Sci. Rep. 8: 10179.

Murayama, J. 1934. Notes on the Ipidae (Coleoptera) from Kiushu. Annot. Zool. Jpn. 14: 287–300.

O'Donnell, K., H. Corby Kistler, E. Cigelnik, and R. C. Ploetz. 1998. Multiple evolutionary origins of the fungus causing Panama disease of banana: Concordant evidence from nuclear and mitochondrial gene genealogies. Proc. Natl. Acad. Sci. USA. 95: 2044–2049.

Rabaglia, R. J., S. A. Dole, and A. I. Cognato. 2006. A review of the *Xyleborina* (Coleoptera: Curculionidae: Scolytinae) in America north of Mexico, with an illustrated key. Ann. Entomol. Soc. Am. 99: 1034–1056.

Schedl, K. E. 1979. Der Typen der Sammlung Schedl Familie Scolytidae (Coleoptera). Kataloge der wissenschaftlichen Sammlungen des Naturhistorisches Museum Wien. Entomologie 3(2): 1–286.

Smith, S. M., and A. I. Cognato. 2014. A taxonomic monograph of Nearctic *Scolytus* Geoffroy (Coleoptera, Curculionidae, Scolytinae). ZooKeys 450: 1–182.

Smith, S. M., R. A. Beaver, and A. I. Cognato. 2018a. New synonymy, new combinations and other taxonomic changes in Japanese xyleborine ambrosia beetles (Coleoptera: Curculionidae: Scolytinae). Zootaxa. 4521: 391–403.

Smith, S.M., R. J. Rabaglia, R. A. Beaver, A. I. Cognato, and P. Thu. 2018b. Attraction of ambrosia beetles (Curculionidae: Scolytinae) to semiochemicals in Vietnam with new records and a new species. Coleopterists Bull. 72: 838–844.

Storer, C., A. Payton, S. McDaniel, B. Jordal, and J. Hulcr. 2017. Cryptic genetic variation in an inbreeding and cosmopolitan pest, *Xylosandrus crassiusculus*, revealed using ddRADseq. Ecol. Evol. 7: 10974–10986.

Stouthamer, R., P. Rugman-Jones, P. Q. Thu, A. Eskalen, T. Thibault, J. Hulcr, L. -J. Wang, B. H. Jordal, C. -Y. Chen, M. Cooperband, *et al*. **2017**. Tracing the origin of a cryptic invader: phylogeography of the *Euwallacea fornicatus* (Coleoptera: Curculionidae: Scolytinae) species complex. Agr. Forest Entomol. 19: 366–375.

Swofford, D. L. 2002. PAUP*. Phylogenetic Analysis Using Parsimony (*and Other Methods). Version 4. Sinauer Associates, Sunderland, MA.

Weidner, H. 1976. Die Entomologischen Sammlungen des Zoologischen Instituts und des Zoologischen Museums der Universität Hamburg. IX. Teil, Insecta VI. Mitteilungen aus dem Hamburgischen Zoologischen Museum und Institut, Hamburg, Germany, 73: S87–S264.

Wuest, C. E., T. C. Harrington, S. W. Fraedrich, H. Y. Yun, and S. S. Lu. 2017. Genetic variation in native populations of the laurel wilt pathogen, *Raffaelea lauricola*, in Taiwan and Japan and the introduced population in the United States. Plant Dis. 101: 619–628.

Wood, S. L., and D.E. Bright. 1992. A catalog of scolytidae and platypodidae (coleoptera), part 2: taxonomic index. Great Basin Nat. Mem. 13: 1–1533.

Yeates, D. K., A. Seago, L. Nelson, S. L. Cameron, L. Joseph, and J. W. H. Trueman. 2011. Integrative taxonomy, or iterative taxonomy? Syst. Entomol. 36: 209–217.